Published May 6, 2016

Soil Gas Diffusivity Controls N_2O and N_2 Emissions and their Ratio

Nimlesh Balaine
Tim J. Clough*
Dep. of Soil and Physical Sciences
PO Box 85084
Lincoln Univ.
Lincoln 7647
Canterbury
New Zealand

Mike H. Beare
Steve M Thomas
Esther D. Meenken
New Zealand Institute for Plant and Food Research
Canterbury Agriculture & Science Centre
Gerald St.
Lincoln 7608
Canterbury
New Zealand

Knowledge of soil biological and physical interactions with respect to N_2O and N_2 fluxes is essential to ensure that agricultural land management is environmentally and economically sustainable. This study determined how varying soil relative gas diffusivity (D_p/D_o) affected cumulative N_2O and N_2 fluxes under simulated ruminant urinary-N deposition. Using repacked soil cores, the effects of varying soil bulk density (ρ_b; from 1.1 to 1.5 Mg m^{-3}) and soil matric potential (ψ; −10 to −0.2 kPa) on D_p/D_o were examined in a Templeton silt loam soil (Udic Haplustept) following the application of simulated ruminant urine (700 kg N ha^{-1}). Fluxes of N_2O and N_2, soil inorganic N, pH, and dissolved organic C (DOC) dynamics were monitored over 35 d. Soil D_p/D_o declined as soil bulk density and soil moisture increased. Soil N_2O emissions increased exponentially as D_p/D_o decreased until D_p/D_o equaled 0.005, where upon N_2O fluxes decreased rapidly due to complete denitrification, such that N_2 fluxes reached a maximum of 60% of N applied at a D_p/D_o of <0.005. Regression analysis showed that D_p/D_o was better able to explain the variation in N_2O and N_2 fluxes than water-filled pore space (WFPS) because it accounted for the interaction of soil ρ_b and ψ. This study demonstrates that soil D_p/D_o can explain cumulative N_2O and N_2 emissions from agricultural soils. Under grazed pasture systems, potential exists to reduce the emissions of the greenhouse gas N_2O and significant economic losses of N as N_2 if soil management and irrigation can be maintained to maximize D_p/D_o.

Abbreviations: ε, air-filled porosity; θ_g, gravimetric water content; θ_v, volumetric water content; ρ_b, bulk density; ϕ, total porosity; ψ, matric potential; DOC, dissolved organic C; D_p/D_o, relative gas diffusivity; WFPS, water-filled pore space.

Core Ideas

- **Relative gas diffusivity controls both N_2O and N_2 emissions.**
- **Relative gas diffusivity integrates the effects of soil bulk density and matric potential.**
- **Nitrogen use efficiency is likely to be driven by soil physics.**

Losses of N_2O from agricultural soils represent a minor economic loss at a farm scale, with 1 to 2% of N applied in fertilizer or animal excreta typically emitted as N_2O, but such losses are a major economic loss on a global basis (Delgado, 2002). Agricultural anthropogenic N_2O emissions have a substantial environmental impact due to the role that N_2O plays, both as a greenhouse gas and as a significant contributor to ozone depletion processes in the stratosphere (Ravishankara et al., 2009). Ruminant excreta and fertilizer are primarily responsible for the increased concentration of N_2O in the troposphere (Davidson, 2009), with ruminant urine deposition within intensively managed pasture systems a significant contributor (de Klein et al., 2001). Conversely, emissions of N_2 from agricultural soils to the atmosphere are environmentally benign, but they represent a greater economic loss of N, with more than 20% of N often assumed to be lost as N_2, with such losses reducing the N use efficiency of crops and pastures (Clough et al., 1996, 2001; Delgado, 2002; Mosier et al., 2004; Buckthought et al., 2015). However, a detailed understanding of soil physical conditions that promote N_2 emissions is limited.

Soil Sci. Soc. Am. J.
Open Access article.
doi:10.2136/sssaj2015.09.0350
Received 27 Sept. 2015.
Accepted 1 Feb. 2016
*Corresponding author (Timothy.Clough@lincoln.ac.nz).

Biological pathways for the formation of N_2O and N_2 in soils include nitrification, nitrifier-denitrification, and denitrification (Wrage et al., 2001). Nitrification occurs under aerobic conditions and does not form N_2, but as O_2 levels in the soil decline (<5%), nitrifier-denitrification commences, followed by denitrification if the soil becomes anoxic (Zhu et al., 2013). However, aerobic denitrification can also occur if the microbial community has had prior exposure to short periods of anoxia (Morley et al., 2008). The reduction of N_2O to N_2 is facilitated by the N_2O reductase enzyme, which is sensitive to O_2 and can be inhibited by the presence of O_2 more so than the other enzymes involved in the denitrification cascade, with the degree of sensitivity potentially organism specific (Morley et al. [2008] and references therein).

The ability for a gas to diffuse into, or out of, a soil depends on the D_p/D_o. This is a function of the soil's total porosity (ϕ), which under extreme conditions may be completely filled with water or air. Generally, a soil's porosity is only partially filled with water, with the remaining porosity air-filled, and thus the soil may be described as having WFPS or air-filled porosity (ε) with units of cubic meters water per cubic meters pores or cubic meters air per cubic meters pores, respectively. The WFPS parameter has been commonly used as a predictor for soil N_2O emissions (Dobbie et al., 1999; Dobbie and Smith, 2001). However, the use of WFPS as a predictor for soil N_2O emissions has generally been derived at a single soil ρ_b, and the relationship between these factors becomes distorted when soil ρ_b varies (Farquharson and Baldock, 2008; Balaine et al., 2013; Ball, 2013; Cook et al., 2013). Soil ψ has also been used to try and predict N_2O emissions (Castellano et al., 2010; Van der Weerden et al., 2012), but this does not allow for varying soil ρ_b effects (Balaine et al., 2013). A better predictor of soil N_2O emissions that overcomes both varying soil moisture contents and soil ρ_b effects is D_p/D_o. Demonstration of the relationship between soil D_p/D_o and N_2O emissions has been shown by taking direct measurements of both N_2O emissions and D_p/D_o (McTaggart et al., 2002; Balaine et al., 2013; Petersen et al., 2013) and by comparing calculated D_p/D_o values with measured N_2O emissions (Andersen and Petersen, 2009; Klefoth et al., 2014; Harrison-Kirk et al., 2015). Despite a call for more emphasis to be placed on the interaction of biological and physical soil processes on greenhouse gas emissions, there appears to be only one detailed study to date that has specifically examined the interaction between soil ρ_b and soil ψ on soil D_p/D_o and the effects of this interaction on N_2O emissions (Balaine et al., 2013). Emissions of N_2O were observed to increase exponentially as the value of D_p/D_o declined; however, N_2O emissions declined dramatically if the value of D_p/D_o declined further below a threshold value, presumably as a consequence of N_2 formation (Balaine et al., 2013). However, specifically designed studies aimed at examining the relationship between the relative production of N_2 and N_2O from soil, under varying soil ρ_b and ψ conditions with respect to D_p/D_o, have not been reported. Thus, the objective of the current study was to determine the relative production of N_2 and N_2O from a soil while manipulating ρ_b and ψ to vary D_p/D_o, following a simulated ruminant urine deposition event.

MATERIALS AND METHODS

Experimental Treatments and Setup

Silt loam soil (Templeton silt loam, classified as Typic Immature Pallic according to New Zealand soil classification [Hewitt, 1998]) was collected (0- to 15-cm depth) from the Duncan Block, Lincoln (43°38′0.7″ S lat; 172°29′40″ E long) and was air-dried before sieving (≤2 mm). The soil texture consisted of 23% sand, 52% silt, and 25% clay. Soil C, N, and organic matter contents were 29.5, 2.6, and 50 g kg^{-1}, respectively, and the soil pH was 6.0. After determining the soil gravimetric water content (θ_g), stainless steel cylinders (7.3-cm i.d., 4.1 cm deep) were packed to a constant volume, and a 4.1-cm depth, with soil that had been previously wetted with deionized water to a predetermined moisture content that still allowed for the subsequent addition of a urea solution. This was so the soil moisture contents of the packed soil cores equated with the predetermined WFPS for each of the three experiments, performed at varying levels of ψ with either −10.0, −6.0, or −0.2 kPa (Exp. 1, 2, and 3, respectively). Soil was packed to a constant volume at soil ρ_b values of 1.1, 1.2, 1.3, and 1.4 Mg m^{-3}, and in the −6.0- and −0.2-kPa experiments, an additional soil ρ_b of 1.5 Mg m^{-3} was also included. To obtain a uniform soil ρ_b, the soil cores were compressed uniaxially 1-cm depth at a time. The bottom of each soil core was covered with a fine nylon mesh to prevent soil egress.

For each experiment, a urea solution (A1 or A2) with an N content of 10 g N L^{-1} was used to simulate urine application. The urea in the A1 solution had a ^{15}N enrichment of 50 atom % excess relative to ambient air in Exp. 1 and 40 atom% in Exp. 2 and 3. The A2 urea solution was not ^{15}N enriched. Urea solutions were applied at a rate of N that corresponded to a bovine urine deposition event (700 kg N ha^{-1}; Haynes and Williams, 1993) by pipetting them slowly on to the soil surface (30 mL per soil core). The A1 solution was applied to soil cores that were used to measure the ^{15}N enrichment of the N_2O flux and to determine the N_2 fluxes throughout the 35-d experimental period. The A2 solution was applied to soil cores that were destructively analyzed on Day 1, 7, 14, and 24.

It is recognized that artificial urine does not generate the same N_2O fluxes as ruminant urine (Kool et al., 2006). However, over 70% of the N in urine is present as urea (Bathurst, 1952; Haynes and Williams, 1993), and it is this major component that undergoes hydrolysis and subsequent N transformation. The aim of this study was not to derive N_2O emission factor data but to examine the effects of soil ρ_b, ψ, and D_p/D_o on N_2O and N_2 fluxes under controlled conditions; thus, urea was chosen over ruminant urine so that the N input was both controlled and highly enriched in ^{15}N to facilitate N_2 flux measurements.

A dye penetration test was also performed in the −10-kPa experiment on a separate set of soil cores and was replicated three times for soils at ρ_b of 1.1 to 1.4 Mg m^{-3} to determine the penetration depth of the urea solutions applied under the various lev-

els of soil compaction. Soils were compacted as described above, and then 30 mL of the tracer dye Brilliant Blue FCF (6 g L^{-1} of deionized water) was applied (Flury and Fluhler, 1994). After 24 h, the cores were extruded and sliced into 0.5-cm increments, and the presence or absence of dye at the dorsal surface of each increment was noted.

A soil water retention curve (WRC) was also constructed to determine the soil pore size distribution under the varying levels of compaction. Compacted soils, replicated 4 times, were sequentially drained to varying levels of ψ using tension tables set at −0.5, −1.0, −1.5, −2.0, −3.0, −4.0, −5.0, −6.0, −7.0, −8.0, −9.0, and −10.0 kPa (Romano et al., 2002), while pressure plate apparatus was used at −100, −500, and −1500 kPa. Soil θ_g contents were determined at each value of ψ, and the diameter of the pore sizes filled with water at a given level of ψ were calculated according to Schjønning et al. (2003). Macro-, meso-, and microporosities were defined as being >30 μm, 30 to 0.2 μm, and <0.2 μm, respectively (Walczak et al., 2002). Measurements of soil D_p/D_o were made on Day 1 and 35 as previously described (Balaine et al., 2013).

Gas Sampling, Analyses, and Flux Determinations

To measure the N_2O and N_2 fluxes, the soil cores were taken off the tension tables and were placed into 1-L stainless steel tins equipped with gas-tight lids prefitted with rubber septa. Ambient air samples were taken at time zero, and headspace N_2O samples were taken at 0, 15, and 30 min after sealing the headspace using a 20-mL glass syringe fitted with a 3-way tap and a 25-gauge 0.5- by 16-mm needle (Precision Glide; Becton-Dickinson, Franklin Lakes, NJ). Samples for N_2O and N_2 analyses were transferred into pre-evacuated (−0.1013 MPa) 6- and 12-mL vials (Exetainer; Labco Ltd., Lampeter, UK), respectively. At −10 kPa, N_2O flux sampling was performed on Day 1, 2, 3, 4, 5, 6, 7, 10, 12, 14, 18, 20, 24, 28, 31, and 35 with N_2 sampling performed on Day 4, 7, 20, 24, 31, and 35. For soil cores run at −6.0 and −0.2 kPa, N_2O flux sampling was performed on Day 1, 2, 3, 4, 5, 6, 7, 10, 12, 14, 16, 20, 24, 28, 31, and 35 with N_2 sampling performed on Day 1, 3, 7, 10, 12, 14, 24, 28, and 35. Analyses of N_2O concentrations were performed using an automated gas chromatograph (8610; SRI Instruments, Torrance, CA) interfaced to an autosampler (Gilson 222XL; Gilson, Middleton, WI) as described by Clough et al. (2006). Fluxes of N_2O were calculated as described by Hutchinson and Mosier (1981). An isotope ratio mass spectrometer (Sercon 20/20; Sercon, Cheshire, UK) was used to determine the ^{15}N enrichment of the N_2O and N_2 gases (Stevens et al., 1993) with N_2 fluxes determined according to the equations of Mulvaney and Boast (1986).

Soil Inorganic N, pH, and Dissolved Organic C

Soil cores were destructively analyzed for inorganic N on Day 7, 14, 21, 28, and 35 at −10 kPa and on Day 1, 7, 14, 24, and 35 at both −6.0 and −0.2 kPa. Soil cores were extruded, and the total wet mass of soil was weighed. Soil subsamples were taken to determine θ_g, inorganic N, and DOC. Soil θ_g was determined using 10 g of wet soil and by drying the soil for 24 h at 105°C. Values of θ_g were subsequently used to determine soil ρ_b, ϕ, volumetric water content (θ_v), and ε, while assuming a particle density of 2.65 Mg m^{-3}. Soil inorganic N was determined by extracting a soil subsample with KCl (equivalent to 10 g dry soil: 100 mL of 2 M KCl) by shaking for 1 h. The extract was filtered (Whatman 42) and analyzed for NH_4^+–N, NO_2^-–N, and NO_3^-–N using flow injection analysis as described by Blakemore et al. (1987). Soil surface pH was measured with a flat surface pH electrode before destructive soil core analysis (Broadley James Corp., Irvine CA.). Soil DOC concentrations were determined by extracting soil subsamples using the methods of Ghani et al. (2003) with DOC analyzed on a Shimadzu TOC analyzer (Shimadzu Oceania Ltd., Sydney, Australia).

Statistical Analysis

All statistical analyses were performed using Minitab version 15 (Minitab Inc., State College, PA). Data sets from each experiment were tested for normality (Anderson and Darling, 1952) with residuals plotted versus fits to verify the assumption that the residuals had constant variance. Fluxes of N_2O and N_2 were log transformed (ln[value + 1]) according to Tiedje et al. (1989). One-way ANOVA was used to determine differences among treatments on individual days with soil ρ_b as a factor, and where differences occurred, Tukey's test was used to determine which means were significantly different from one another. A repeated measures ANOVA (general linear model in Minitab) was used to determine the interaction of time and soil ρ_b on N_2O and N_2 data. Regression analyses were performed using Sigmaplot (Systat Software, Inc., San Jose, CA) to assess the relationship between cumulative N_2 and N_2O fluxes with D_p/D_o. Pearson correlation was used to determine the strength and direction of the relationships between soil variables. Figures were prepared using Sigmaplot. Mean and SEM values from multiple experiments were presented in each figure.

RESULTS

Soil Physical and Chemical Properties

As soil ρ_b increased, values of ϕ declined ($p < 0.05$) from 0.58 to 0.47 m^3 m^{-3}. Increasing soil ρ_b also altered the pore size distribution: soil macroporosity (pores with a diameter of >30 μm) as a percentage of total porosity decreased ($p < 0.01$) from 62% at 1.1 Mg m^{-3} to 30% at 1.5 Mg m^{-3}, while both mesoporosity (pores with a diameter of 30–0.2 mm) and microporosity (pores with a diameter of <0.2 mm) increased ($p < 0.01$) by 27 and 6%, respectively (Fig. 1). Progressively increasing soil ρ_b led to a decline ($p < 0.01$) in macroporosity as a percentage of the total soil volume, with the decline equaling 23% at 1.5 Mg m^{-3}, while mesoporosity and microporosity increased by 6 and 2%, respectively, at 1.5 Mg m^{-3}.

In the −10-kPa experiment, values of θ_v increased ($p < 0.05$) from 0.26 m^3 m^{-3} at 1.1 Mg m^{-3} to 0.33 m^3 m^{-3} at 1.4 Mg m^{-3}, and in the −6.0-kPa experiment, values of θ_v also

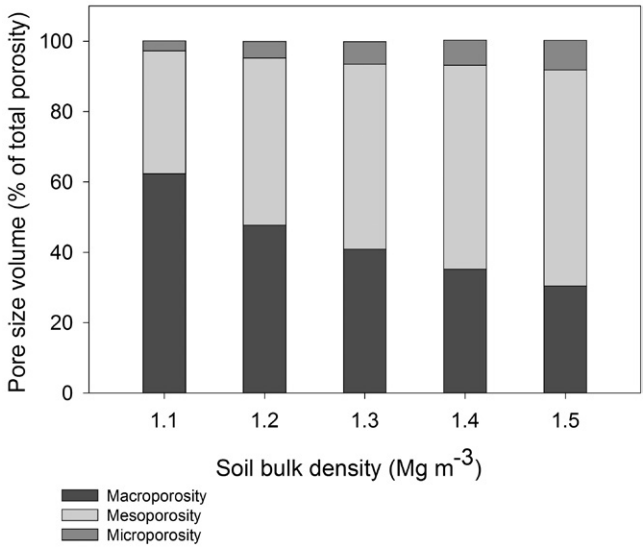

Fig. 1. Soil bulk density-induced changes in soil pore class as a percentage of total soil porosity: macroporosity (diameter of >30 μm), mesoporosity (diameter of 30–0.2 μm), and microporosity (diameter of <0.02 μm).

increased ($p < 0.05$) as soil ρ_b increased from 0.32 $m^3\ m^{-3}$ at 1.1 Mg m^{-3} to 0.38 $m^3\ m^{-3}$ at 1.5 Mg m^{-3} (Table 1). Conversely, in the −0.2-kPa experiment, values of θ_v declined ($p < 0.05$) with increasing soil ρ_b from 0.57 $m^3\ m^{-3}$ at 1.1 Mg m^{-3} to 0.46 $m^3\ m^{-3}$ at 1.5 Mg m^{-3} (Table 1).

Values of ε declined ($p < 0.05$) as soil ρ_b increased in both the −10- and −6.0-kPa experiments from 0.32 $m^3\ m^{-3}$ at 1.1 Mg m^{-3} to 0.14 $m^3\ m^{-3}$ at 1.4 Mg m^{-3} and from 0.27 $m^3\ m^{-3}$ at 1.1 Mg m^{-3} to 0.06 $m^3\ m^{-3}$ at 1.5 Mg m^{-3}, respectively (Table 1). However, in the −0.2-kPa experiment, values of ε remained static at ≤0.01 $m^3\ m^{-3}$ regardless of the soil ρ_b treatment (Table 1).

Increasing soil ρ_b from 1.1 to 1.4 Mg m^{-3} increased WFPS ($p < 0.05$) in experiments at −10 and −6.0 kPa from 44 to 70% and 54 to 85%, respectively; however, at −0.2 kPa, WFPS remained constant at ≥98% regardless of the soil ρ_b (Table 1).

Measures of D_p/D_o in all experiments showed the day of measurement had no impact on values attained ($p > 0.05$). Under near saturated conditions at a soil ψ of −0.2 kPa, D_p/D_o values equaled zero regardless of soil ρ_b treatment (Table 1). Under soil ψ values of −10 kPa and −0.6 kPa, Exp. 1 and 2, respectively, D_p/D_o values declined ($p < 0.05$) with increasing soil ρ_b treatment from 0.063 to 0.008 at −10 kPa and from 0.014 to 0.0014 at −6.0 kPa (Table 1). The average dye penetration depth decreased from 4 to 3 cm as soil ρ_b increased from 1.1 to 1.4 Mg m^{-3}, respectively (Table 1).

Within a day of urea application, soil surface pH became elevated (8–9) at −6.0 and −0.2 kPa. By Day 7, soil pH remained between 8 and 9 in Exp. 1 at −10 kPa and also in the lowest soil ρ_b treatments (1.1 and 1.2 Mg m^{-3}) at −6.0 kPa and at the lowest soil ρ_b treatment (1.1 Mg m^{-3}) within the −0.2-kPa experiment. In all other treatments, regardless of experimental kPa level, soil pH continued to decline. There were no differences in soil pH due to soil ρ_b treatment in the urea-treated cores at −10 kPa. Exceptions to this steady decline in soil surface pH were treatments that were compacted to 1.4 and 1.5 Mg m^{-3} at −0.2 kPa, where soil pH increased between Day 24 and 35, and the 1.1 and 1.5 Mg m^{-3} treatments at −6.0 kPa, where the soil pH declined at a slower rate (Fig. 2).

Table 1. Total soil porosity (ϕ), dye penetration depth, soil volumetric water content (θ_v), soil water-filled pore space (WFPS), soil air-filled pore space (ε), and soil relative gas diffusivity (D_p/D_o).

Variable	Matric potential	Soil bulk density level‡					Significance
		1.1	1.2	1.3	1.4	1.5	
	kPa	Mg m^{-3}					
Soil ϕ, m^3 air m^{-3} soil	All kPa levels	0.58 (0)	0.55 (0)	0.51 (0)	0.47 (0)	0.43 (0)	**
Dye penetration depth, cm	−10 kPa (Exp. 1)	4 a (0)	3.6 ab (0.25)	3.3 b (0.29)	3.1 b (0.48)	ND§	**
Soil θ_v, m^3 water m^{-3} soil	−10 kPa (Exp. 1)	0.26 c (0.006)	0.28 b (0.006)	0.31 a (0.015)	0.33 a (0.004)	ND	**
WFPS, %		44 d (0.96)	51 c (1.16)	61 b (2.95)	70 a (0.91)	ND	**
Soil ε, m^3 air m^{-3} soil		0.32 a (0.006)	0.27 b (0.006)	0.20 c (0.015)	0.14 d (0.004)	ND	**
D_p/D_o Day 1		0.063 a (0.008)	0.037 b (0.012)	0.026bc (0.007)	0.008 c (0.005)	ND	**
D_p/D_o Day 35		0.061 a (0.007)	0.039 b (0.004)	0.026 c (0.003)	0.013 d (0.003)	ND	**
Soil θ_v (m^3 water m^{-3} soil)	−6.0 kPa (Exp. 2)	0.32 d (0.006)	0.35 c (0.009)	0.37 b (0.006)	0.39 a (0.008)	0.38 ab (0.005)	**
WFPS (%)		54 a (0.98)	64 b (1.66)	73 c (1.21)	85 d (1.77)	89 e (1.24)	**
Soil ε (m^3 air m^{-3} soil)		0.27 a (0.005)	0.19 b (0.009)	0.14 c (0.006)	0.07 d (0.008)	0.06 e (0.005)	**
D_p/D_o Day 7		0.014 a (0.002)	0.01 b (0.001)	0.007 c (0.0004)	0.004 d (0.0002)	0.002 e (0.0002)	**
D_p/D_o Day 35		0.01 a (0.001)	0.007 b (0.0002)	0.005 c (0.0001)	0.004 d (0.0002)	0.0014 e (0.0002)	**
Soil θ_v (m^3 water m^{-3} soil)	−0.2 kPa (Exp. 3)	0.57 a (0.008)	0.54 b (0.002)	0.50 c (0.006)	0.46 d (0.009)	0.43 e (0.006)	**
WFPS (%)		98 a (1.37)	99 a (0.44)	98 a (1.32)	98 a (1.9)	99 a (1.38)	NS†
Soil ε (m^3 air m^{-3} soil)		0.01 a (0.008)	0.006 a (0.002)	0.01 a (0.007)	0.008 a (0.009)	0.005 a (0.006)	NS
D_p/D_o Day 7		0	0	0	0	0	NS

** $p < 0.01$.

† NS, not significant.

‡ Values in a row that do not share a common letter are significantly different ($p < 0.01$, Tukey's test); $n = 4$ for all tests with the exception of blue dye tests where $n = 3$. The SD appears in parentheses.

§ ND, not determined.

Soil DOC peaked at 703 μg g^{-1} soil on Day 7 at −10 kPa, exceeding values found in the control soils (21 to 44 μg g^{-1} soil), and declined with time with lower values ($p < 0.05$) in the highest soil ρ_b treatments until Day 21 (Fig. 2). At −6.0 kPa, soil DOC increased under urea application to peak at 566 μg g^{-1} soil on Day 1, again in excess of control soil concentrations of ≤27 μg g^{-1} soil. The DOC concentrations under urea at −6.0 kPa were highest under the lowest soil ρ_b treatment, where the rate of decline in DOC was also slower ($p < 0.01$). With soil ψ set at −0.2 kPa, the soil DOC concentrations also peaked within a day of urea application at 710 μg g^{-1} soil, with values higher ($p < 0.01$) under the lowest soil ρ_b treatments until Day 15; thereafter, values remained relatively stable (Fig. 2). In all experiments, soil DOC concentrations were strongly correlated to soil pH ($r = 0.85–0.96$) on Day 1 or 7. Soil DOC concentrations correlated with dye penetration depth on Day 7 ($r = 0.84$; $p < 0.01$) and 21 ($r = 0.61$; $p < 0.01$) at −10 kPa.

At −10 kPa, the soil NH_4^+–N concentrations were highest on Day 7, 1178–979 μg g^{-1} soil, before declining over time with no effect of soil ρ_b treatment (Fig. 3). Concentrations of NH_4^+–N became elevated by Day 1 at −6.0 kPa, 1400–1055 μg g^{-1} soil, before declining over time but with higher ($p < 0.05$) concentrations at a soil ρ_b of 1.1 Mg m^{-3} on all days (Fig. 3). In the −0.2-kPa experiment, soil NH_4^+–N concentrations under urea were also at their peak on Day 1 (1490–994 μg g^{-1} soil) again with higher ($p < 0.01$) concentrations in the lowest soil ρ_b treatments of 1.1 and 1.2 Mg m^{-3} on all days (Fig. 3).

At −10 kPa NO_2^-–N concentrations were <0.4 μg g^{-1} soil in the control but became elevated ($p < 0.05$) following urea application with peak concentrations in the 1.1 and 1.2 Mg m^{-3} treatments of 54 μg g^{-1} soil on Day 21 (Fig. 3). In the −6.0 kPa experiment, NO_2^-–N concentrations in the control treatments were ≤0.1 μg g^{-1} soil. However, under urea at −6.0 kPa, an interaction between time with soil ρ_b resulted in NO_2^-–N concentrations increasing by Day 7 in all treatments but with the rate of increase reducing as soil ρ_b increased. After Day 7, NO_2^-–N concentrations continued to increase in the 1.1 Mg m^{-3} treatment until Day 15 (11 μg g^{-1} soil) at which point they declined, decreased in the 1.2 to 1.4 Mg m^{-3} treatments, but continued to increase in the 1.5 Mg m^{-3} treatment until Day 24 (14 μg g^{-1} soil) before then declining (Fig. 3). In the experiment at −0.2 kPa, control treatments again had low NO_2^-–N concentrations (<0.1 μg g^{-1} soil), and an interaction between time and soil ρ_b also occurred following urea application: NO_2^-–N concentrations peaked on Day 7 in treatments of 1.1 to 1.4 Mg m^{-3}, thereafter NO_2^-–N concentrations declined in treatments of 1.1 to 1.3 Mg m^{-3} until Day 14 before increasing again to be 13 to 21 μg g^{-1} soil by Day 35, while at 1.4 Mg m^{-3} NO_2^-–N concentrations continued to decline equaling those in the controls by Day 24 (Fig. 3). In the 1.5 Mg m^{-3} treatment, NO_2^-–N concentrations peaked at Day 14 (23 μg g^{-1} soil) before declining to values seen in the controls at Day 35 (Fig. 3).

Soil NO_3^-–N concentrations within the −10-kPa experiment gradually increased to reach 295 to 329 μg g^{-1} soil fol-

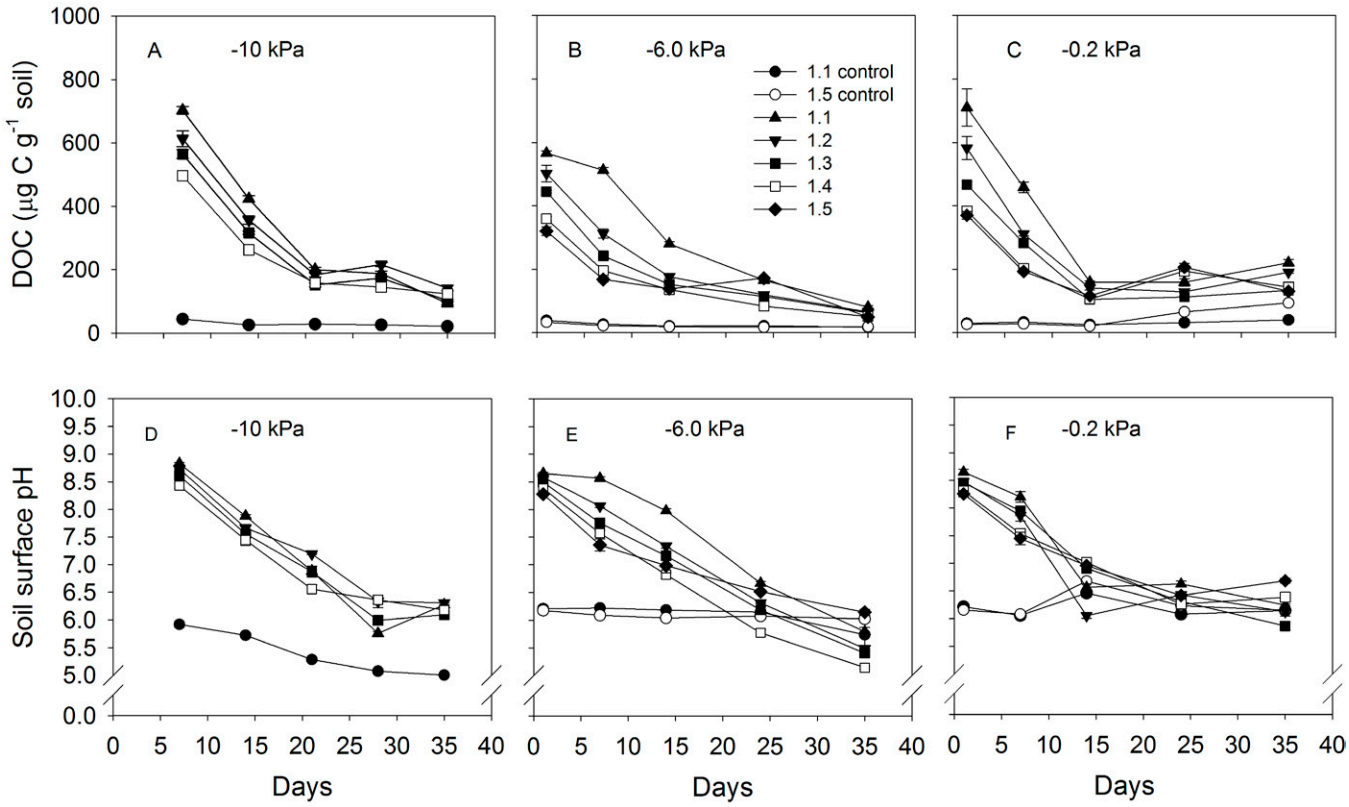

Fig. 2. Mean soil dissolved organic C (DOC) concentrations (a, b, c) and surface soil pH (d, e, f) over time following soil compaction and urea solution application for the three experiments performed at −10, −6.0, and −0.2 kPa. Numerals in the legend indicate soil bulk density (ρ_b) treatments applied (Mg m^{-3}). Error bars = SEM; $n = 4$.

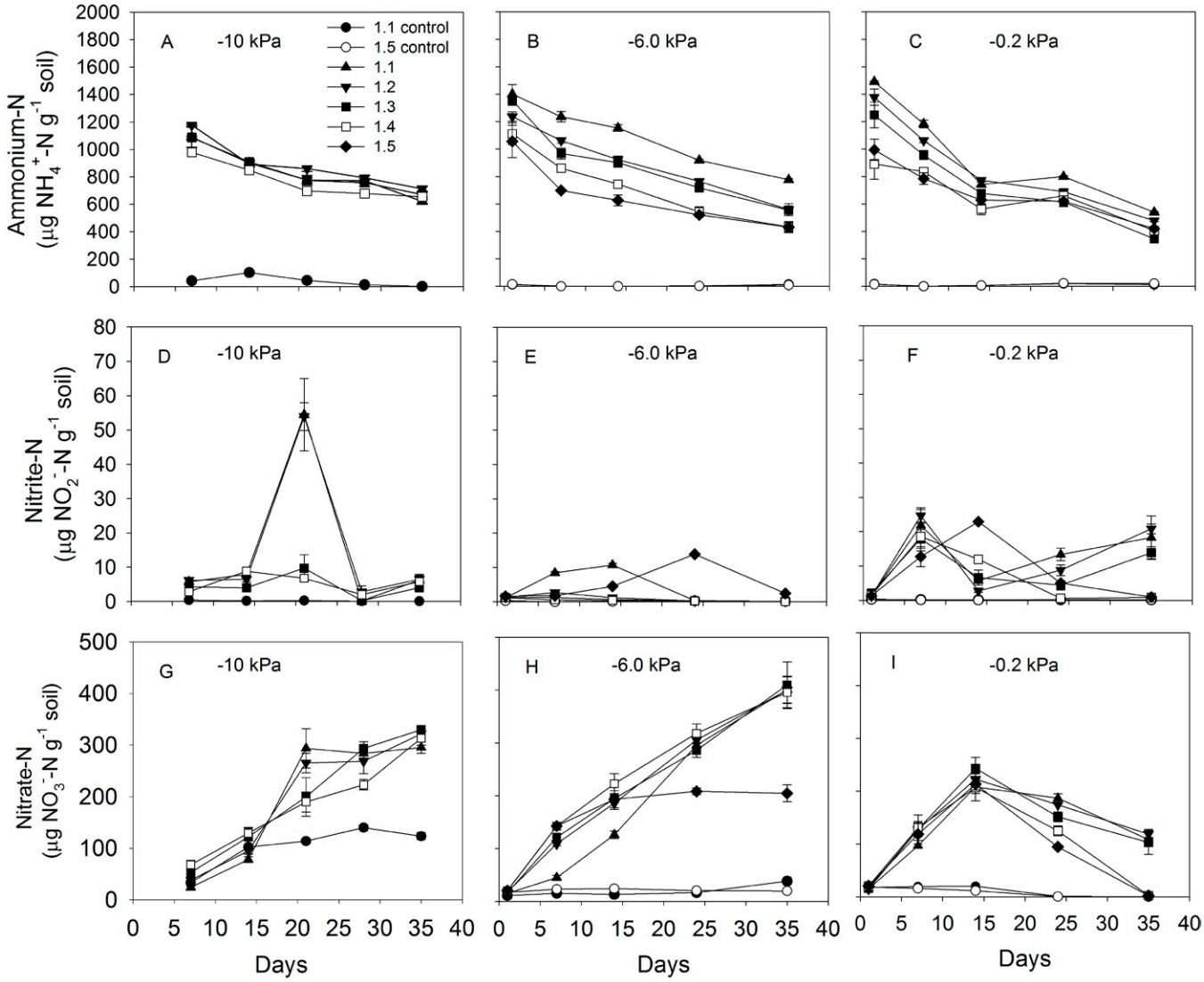

Fig. 3. Mean soil NH_4^+–N (a, b, c), NO_2^-–N (d, e, f), and NO_3^-–N (g, h, i) following soil compaction and urea solution application for the three experiments performed at −10, −6.0, and −0.2 kPa. Numerals in the legend indicate soil bulk density (ρ_b) treatments applied (Mg m^{-3}). Error bars = SEM; *n* = 4.

lowing urea application with no consistent effects of the soil ρ_b treatments, while in the control treatments, soil NO_3^-–N concentrations were lower ($\leq$123 μg g^{-1} soil) from Day 14 (Fig. 3). At −6.0 kPa, soil NO_3^-–N concentrations in the control treatment remained relatively low and stable ($\leq$25 μg g^{-1} soil), but urea-treated soil cores produced an interaction between time and soil ρ_b ($p < 0.01$) with NO_3^-–N concentrations steadily increasing to approximately 400 μg g^{-1} soil but with a slower rate of increase on Day 7 and 14 at 1.1 Mg m^{-3} compared to the 1.2 to 1.4 Mg m^{-3} treatments and with no increase in the 1.5 Mg m^{-3} treatment after Day 15 where concentrations remained constant at approximately 200 μg g^{-1} soil (Fig. 3). In Exp. 3, set at −0.2 kPa, soil NO_3^-–N concentrations at Day 35 were relatively low when compared with Exp. 1 and 2 (Fig. 3). Again, NO_3^-–N concentrations were low in the controls, $\leq$12 μg g^{-1} soil (Fig. 3), but they increased in all soil ρ_b treatments following urea application until Day 14 ($\leq$243 μg g^{-1} soil), after which a soil ρ_b × time interaction ($p < 0.01$) produced a faster decline in soil NO_3^-–N concentrations in the 1.4 and 1.5 Mg m^{-3} treatments, which reached 0 μg g^{-1} soil by Day 35, than in the 1.1 to 1.3 Mg m^{-3} treatments, which were approximately 100 to 120 μg g^{-1} soil at Day 35.

Soil Nitrous Oxide and Dinitrogen Fluxes and their Ratios and Relationships with Soil Physical Parameters

Daily fluxes of N_2O-N were low in the controls at −10 kPa (<0.13 mg N_2O-N m^{-2} h^{-1}) but increased following urea application ranging from 0.01 to 10.3 mg N_2O-N m^{-2} h^{-1}, with higher fluxes after Day 8 (Fig. 4) and with cumulative N_2O emissions increasing ($p < 0.01$) from 0.05 to 2.14% of N applied as soil ρ_b increased (Fig. 4). At −6.0 kPa, fluxes of N_2O-N were again relatively low in the controls (<0.3 mg N_2O-N m^{-2} h^{-1}) but there was an interaction between time and soil ρ_b in the urea-treated cores: fluxes increased sharply at Day 7 and 8 in the 1.1 to 1.3 Mg m^{-3} treatments, after which these fluxes

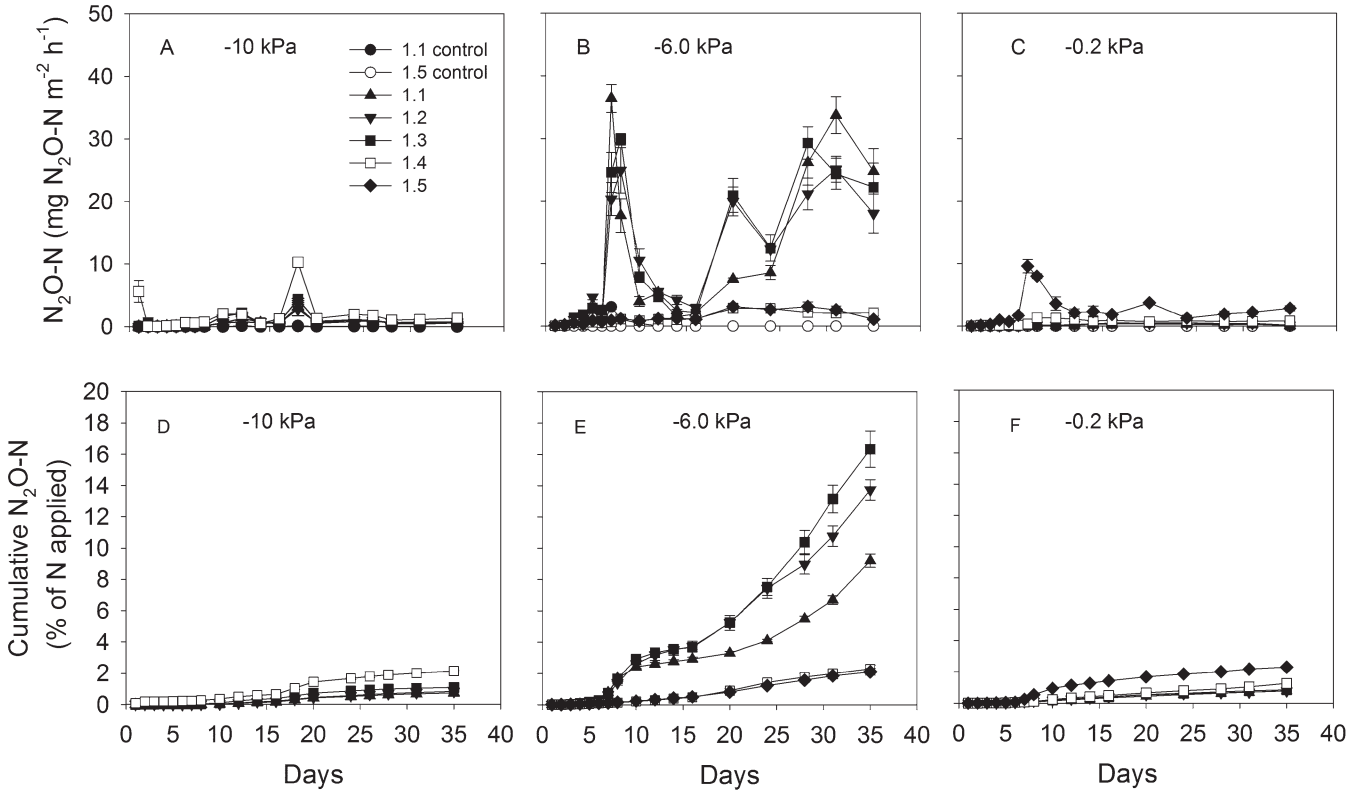

Fig. 4. Mean daily N_2O-N fluxes (a, b, c) and cumulative N_2O-N fluxes (d, e, f) from soil cores over time following soil compaction and urea solution application for the three experiments performed at −10, −6.0, and −0.2 kPa. Numerals in the legend indicate soil bulk density (ρ_b) treatments applied (Mg m^{-3}). Error bars = SEM; *n* = 4.

declined until Day 16 when they increased through to Day 35; fluxes of N_2O-N from the 1.4 and 1.5 Mg m^{-3} remained relatively low throughout the 35 d (Fig. 4). The cumulative N_2O-N fluxes at −6.0 kPa, as a percentage of N applied, reflected these trends with ≤2.2% at 1.4 and 1.5 Mg m^{-3} and 9 to 16.3% recovered in the 1.1 to 1.3 Mg m^{-3} treatments (Fig. 4). In the −0.2-kPa experiment, N_2O-N fluxes were higher at 1.4 and 1.5 Mg m^{-3} with a maximum of 9.5 mg N_2O-N m^{-2} h^{-1} on Day 7, while fluxes in the 1.1 to 1.3 Mg m^{-3} treatments remained at <1 mg N_2O-N m^{-2} h^{-1} (Fig. 4). Reflecting these trends, cumulative N_2O-N fluxes at −0.2 kPa increased after Day 7 and ranged from 0.8 to 2.3% of N applied in the 1.1 and 1.5 Mg m^{-3} soil ρ_b treatments, respectively (Fig. 4). Changes in atom % ^{15}N enrichment of the N_2O-N over time generally followed the same trend in each experiment, increasing for 15 d before stabilizing at approximately 45, 36, and 36 atom % at −10, −6.0, and −0.2 kPa, respectively.

In the −10 kPa experiment, the average N_2–N fluxes ranged from 0.55 to 4.9 mg m^{-2} h^{-1} and were generally higher at ≥1.3 Mg m^{-3} (Fig. 5), and thus cumulative N_2–N fluxes equated to 0.06 to 4.97% of N applied after 35 d (Fig. 5). Under wetter soil conditions at −6.0 kPa, increasing soil ρ_b resulted in higher daily N_2–N fluxes, with these N_2–N fluxes driven by a time × soil ρ_b interaction ($p < 0.01$) in the 1.5 Mg m^{-3} treatment between Day 14 and 28 (Fig. 4). Cumulative N_2–N fluxes at −6.0 kPa increased with increasing soil ρ_b to range from 8.3 to 50.0% of N applied in the 1.1 to 1.5 Mg m^{-3} treatments, respectively (Fig. 5). In the experiment performed at −0.2 kPa, soil N_2–N fluxes were again influenced by a time × soil ρ_b interaction ($p < 0.01$), where more rapid increases and prolonged fluxes occurred in the 1.4 to 1.5 Mg m^{-3} treatments (Fig. 5). After 35 d, mean cumulative N_2–N emissions as a percentage of N applied increased with soil ρ_b ranging from 16 to 60% at 1.1 and 1.5 Mg m^{-3} treatments, respectively (Fig. 5). Mean values of $^{15}X_N$ (the mole fraction of ^{15}N in the N pool from which N_2 was derived) were 0.43, 0.29, and 0.32 in the −10-, −6.0-, and −0.2-kPa experiments, respectively.

Pooling data from the three experiments and plotting cumulative N_2O-N fluxes as a percentage of N applied vs. WFPS showed no clear relationship (Fig. 6). However, when plotted against D_p/D_o the N_2O-N flux as a percentage of N applied increased sequentially with increasing soil ρ_b within the −10-kPa treatment, and then when the soil moisture was increased to −6.0 kPa, the N_2O-N flux as a percentage of N applied lifted dramatically, but sequentially, until a soil ρ_b of 1.3 was reached; thereafter, the N_2O-N flux declined and remained low for all remaining soil moisture by soil ρ_b treatment combinations (Fig. 6). This point of rapid decline in the N_2O-N flux equated to a D_p/D_o value of 0.005 (Fig. 6). When N_2–N fluxes as a percentage of N applied were plotted against WFPS, no clear relationship emerged (Fig. 6). But when plotted against D_p/D_o, there was a sequential increase in the N_2–N flux as a percentage of N applied that was dependent on the interaction of ψ and soil ρ_b, with peak N_2–N fluxes occurring at a D_p/D_o value of <0.005 (Fig. 6). However, of note was the fact that at −0.2 kPa, the trend

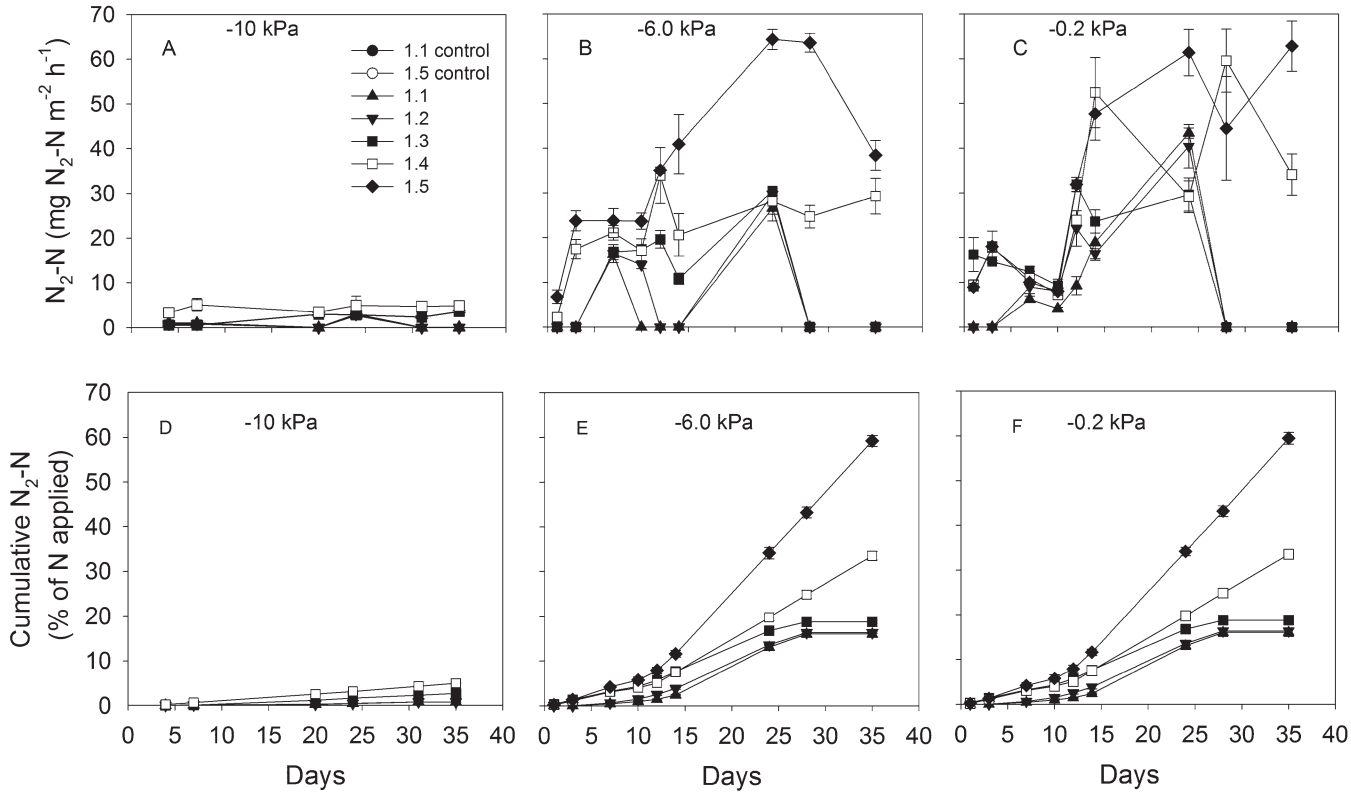

Fig. 5. Mean daily N_2–N fluxes (a, b, c) and cumulative N_2–N fluxes (d, e, f) from soil cores over time following soil compaction and urea solution application for the three experiments performed at −10, −6.0, and −0.2 kPa. Numerals in the legend indicate soil bulk density (ρ_b) treatments applied (Mg m^{-3}). Error bars = SEM; n = 4.

for fluxes to increase sequentially with increasing soil ρ_b within a given ψ was reversed: at −0.2 kPa N_2–N fluxes declined as soil ρ_b increased (Fig. 6). When the ratio of N_2–N/N_2O-N was plotted versus D_p/D_o data, the ratio increased rapidly at a D_p/D_o value of <0.005 (Fig. 6).

Regression analysis explained 88% of the variation in the relationship between log-D_p/D_o, when D_p/D_o was >0.005, and the log-cumulative N_2O-N flux (Fig. 7), with a respective value of 44% when plotted against log WFPS. Likewise, 93% of the variation in the relationship between log D_p/D_o, when D_p/D_o was >0, and the log-cumulative N_2–N flux, could be explained by linear regression (Fig. 7), with a respective value of 83% when plotted against log WFPS.

DISCUSSION

Soil Chemical and Physical Characteristics

Increases in the percentages of meso- and microporosities with increasing soil ρ_b allowed a given soil volume to retain more water at a given level of soil ψ, which in turn produced the observed decline in ε as soil ρ_b increased in the −10- and −6.0-kPa experiments. At −0.2 kPa, however, the soil was effectively saturated regardless of the soil ρ_b treatment applied. The effect of increasing soil ρ_b on soil pore size distribution and the associated decreases in ε and ϕ explain the decline in D_p/D_o with increasing soil ψ since D_p/D_o is a function of both ε and ϕ (Millington and Quirk, 1961; Moldrup et al., 2000), and the diffusion of O_2 through water is several orders of magnitude below that in air (Rolston and Moldrup, 2002). Values of ε, ϕ, and D_p/D_o were comparable to previously reported values for repacked soil cores (Balaine et al., 2013).

Elevated soil pH values observed under the urea treatments occurred as a result of urea hydrolysis forming CO_3^{2-} ions, which further hydrolyzed to produce HCO_3^- and OH^- ions (Avnimelech and Laher, 1977). Subsequent declines in soil pH occur as a result of NH_3 volatilization (Avnimelech and Laher, 1977) and nitrification (Prosser, 2012).

Soil NO_3^-–N concentrations are of course net values due to inputs from nitrification and losses via denitrification processes (nitrifier denitrification and/or denitrification), the latter being a function of the soil's aeration status, which is indicated by D_p/D_o. Stepniewski (1981) found that when the D_p/D_o values ranged from 0.02 to 0.005, anaerobic soil conditions prevailed. However, the actual occurrence of anaerobic conditions at a given D_p/D_o value will still depend on the soil's O_2 demand (Petersen et al., 2013). At −10 kPa, D_p/D_o values were >0.02 until soil ρ_b increased to 1.4 Mg m^{-3} when the value equaled 0.008, indicating anaerobic conditions may have occurred in this treatment despite soil NO_3^-–N concentrations continuing to increase over time in all soil ρ_b treatments. The cumulative loss of N_2 at −10 kPa in both the 1.3 and 1.4 Mg m^{-3} treatments ($\leq$5%) confirms denitrification processes did occur but at a D_p/D_o value of $\leq$0.026. At −6.0 kPa, declines in net soil NO_3^-–N concentrations over time were only observed at 1.5 Mg m^{-3}, where denitrification processes clearly exceeded NO_3^-–N sup-

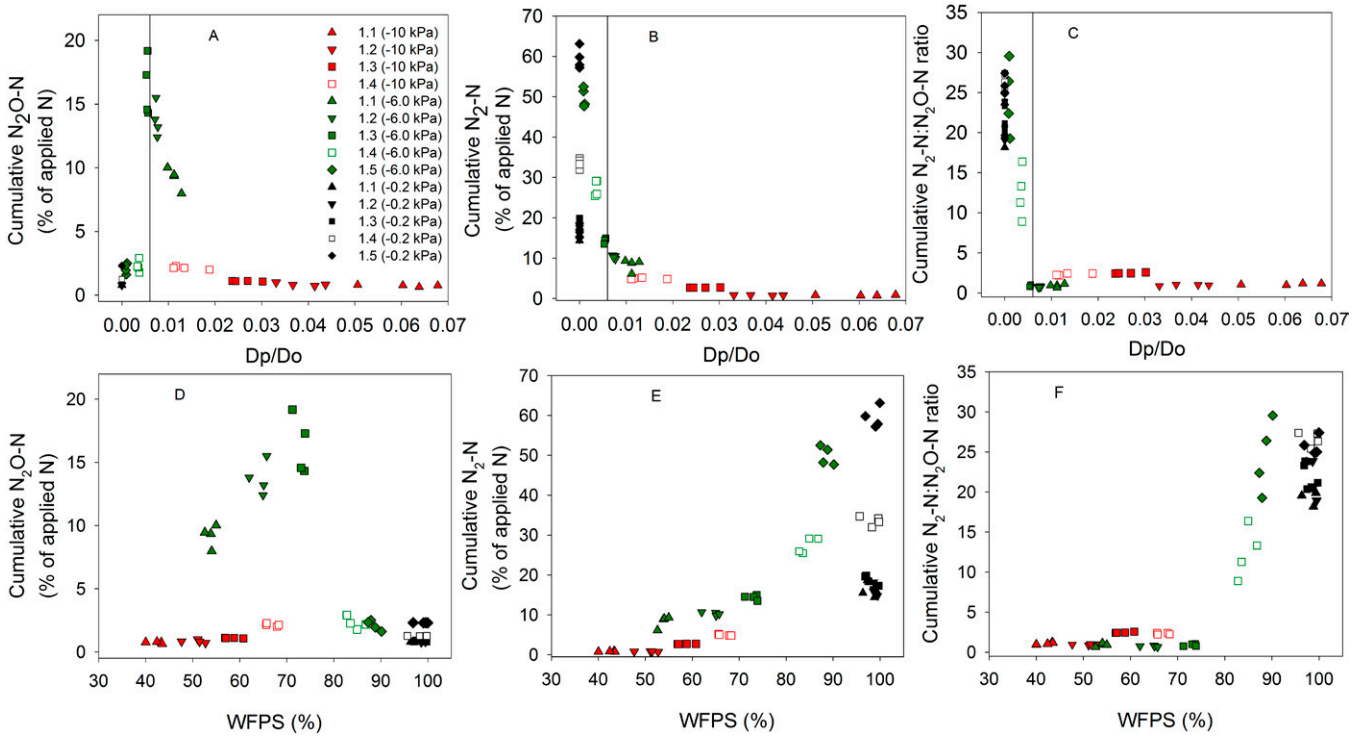

Fig. 6. Pooled cumulative N_2O-N flux, cumulative N_2–N flux, and cumulative flux ratio data from the three experiments performed at −10, −6.0, and −0.2 kPa plotted vs. relative gas diffusivity (D_p/D_o; a, b and c), where the vertical line at a D_p/D_o of 0.006 is the critical value found by Balaine et al. (2013), and plotted vs. water-filled pore space (WFPS; d, e, f). Numerals in legend indicate soil bulk density (ρ_b) treatments applied (Mg m^{-3}) with relative matric potential (ψ) experiment in brackets. Data points are individual replicates.

ply. This was despite the fact that D_p/D_o values were within the anaerobic range given by Stepniewski (1981) at all levels of soil ρ_b. The fluxes of N_2O and N_2 at −6.0 kPa, which were higher than those at −10 kPa, confirmed that denitrification processes occurred with the contribution of the N_2O-N flux reduced at 1.4 and 1.5 Mg m^{-3} due to further reduction of N_2O to N_2.

Of note in the −6.0-kPa experiment was the rapid increase in the N_2O-N flux on Day 7 in soil ρ_b treatments of 1.1 to 1.3 Mg m^{-3}. Fluxes of N_2O are strongly linked to NO_2^- intensity in the soil, a function of its concentration and duration (Maharjan and Venterea, 2013). Thus, this initial period of elevated N_2O-N fluxes at 1.1 to 1.3 Mg m^{-3} was most likely a result of the formation and increasing concentration of NO_2^- in the soil, which was elevated in these soil ρ_b levels on Day 7, the same day N_2O fluxes increased. This effect has been previously observed following bovine urine application to pasture soil (Clough et al., 2009). The reason these N_2O-N fluxes were elevated for approximately 10 d was most likely due to bacterial nitrifiers having to increase nitrite oxidoreductase (*nxr*A) abundance. Venterea et al. (2015) found that it required 10 d for the abundance of *nxr*A to increase following the addition of urea (1000 mg N kg^{-1} soil) to soils at 85% of field capacity. Clough et al. (2009) also observed significant growth in *nxr*A gene copy abundance after soil NO_2^- concentrations peaked 8 to 10 d following bovine urine application to pasture soil.

This strong, potentially NO_2^-–induced N_2O flux at Day 7 onward was not seen at −6.0 kPa in the 1.4 and 1.5 Mg m^{-3} treatments due to further reduction of N_2O to N_2, a consequence of the soil being in the anaerobic range ($D_p/D_o \leq 0.004$) in these treatments. The second period of elevated N_2O fluxes at −6.0 kPa was due to denitrification processes. At −10 kPa, D_p/D_o values were higher and the soil was too well aerated for NO_2^- to form N_2O to the same extent via denitrification processes, while at −0.2 kPa, a peak in the N_2O-N flux of shorter duration only occurred at 1.5 Mg m^{-3}, again at Day 7.

At −0.2 kPa, the D_p/D_o values were effectively zero once the urea solution had been applied. While O_2 will still have penetrated to a shallow depth at the soil surface, the denitrification processes were of a sufficiently high rate that NO_3^- concentrations declined at all levels of soil ρ_b with lower N_2O-N fluxes due to a more complete reduction of the N_2O as evidenced by the relatively high N_2 fluxes.

Relationship of N_2O-N and N_2–N fluxes with Water-filled Pore Space and D_p/D_o

Pooling the data from the three experiments and plotting both the cumulative N_2O-N and N_2–N fluxes and their ratios against D_p/D_o (Fig. 6) allows the interactive effects of soil ρ_b and ψ to be integrated so that the progressive effect of diminishing D_p/D_o on the magnitude of the N_2O-N and N_2–N fluxes is observed. The N_2O-N fluxes were observed to increase in a sequential fashion, from low to high soil ρ_b and from dry (−10 kPa) to wet (−6.0 kPa), with no such order observed when soils were saturated. A similar sequence was observed for the N_2–N fluxes; however, this sequential order was reversed at −0.2 kPa with higher N_2–N fluxes in the 1.5 Mg m^{-3} treatment. This resulted from applying urea solutions after soil compaction so that the urea solution did not penetrate as far into the soil as in the

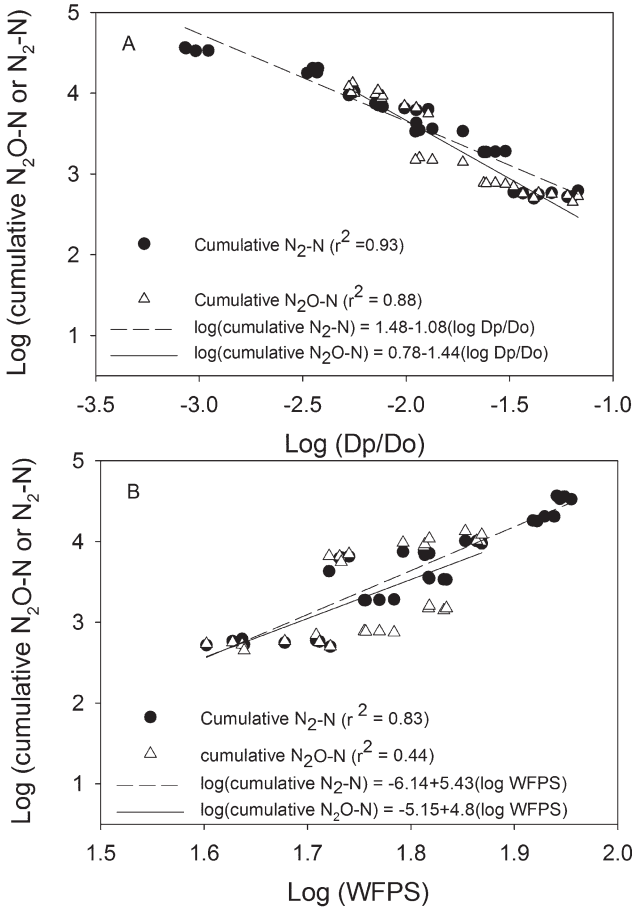

Fig. 7. Regression of cumulative N_2O-N and cumulative N_2–N fluxes, expressed as their respective log values, vs. the log of relative gas diffusivity (D_p/D_o). Cumulative N_2O-N fluxes are plotted for D_p/D_o values of ³0.005 while cumulative N_2–N fluxes are plotted for D_p/D_o values of >0. Data points are individual replicates. WFPS, water-filled pore space.

less compacted treatments, as evident from the blue dye test. Thus, at 1.5 Mg m^{-3}, the diffusive pathway for N_2 was shorter, which helps to explain the higher N_2–N fluxes at 1.5 Mg m^{-3}. Conversely, fluxes in the saturated soils at soil ρ_b of $\leq$1.4 may have been lower as a result of the urea solution penetrating deeper so that the ensuing N_2 produced was entrapped deeper in the soil cores and unable to readily diffuse out (Letey et al., 1980; Clough et al., 2001).

The pooled data set enables a comparison of the cumulative fluxes against WFPS, a readily obtained soil variable often used to predict or explain soil N_2O emissions (e.g., Linn and Doran, 1984). However, as Farquharson and Baldock (2008) noted, WFPS by the very nature of its derivation does not integrate the interactive effects of varying soil ρ_b and ψ on soil gaseous emissions. This experiment reinforces the comments of Farquharson and Baldock (2008). While previous studies have shown strong relationships between soil ψ and N_2O emissions (Petersen et al., 2008; Castellano et al., 2010; Van der Weerden et al., 2012), such relationships are not robust when soil ρ_b also varies (Balaine et al., 2013). Measuring N_2O fluxes from a factorial experiment where soil cores varied in both soil ρ_b and ψ 4 d after saturating soil cores with a NO_3^- solution, Balaine et al. (2013) demonstrated that N_2O fluxes were poorly explained by WFPS but that a strong linear relationship ($p < 0.01$; $r^2 = 0.82$) between log-N_2O-N flux and log D_p/D_o, which encapsulated the variation in both ρ_b and ψ, explained the variation in N_2O fluxes well. The current results further demonstrate that this relationship holds for cumulative fluxes (Fig. 7), even after monitoring N_2O-N fluxes over a 35-d period during a complete inorganic N transformation sequence from urea hydrolysis through to NO_3^- removal via denitrification processes.

Balaine et al. (2013) defined a critical D_p/D_o value (0.006) where maximum measured N_2O-N fluxes occurred. Similarly, in the current study N_2O-N fluxes increased with decreasing D_p/D_o values until D_p/D_o equated to a very similar critical value (0.005), and as in Balaine et al. (2013), N_2O-N fluxes declined dramatically below the critical D_p/D_o value (Fig. 6). This decline in N_2O-N flux can now be confirmed as being the result of N_2 production and possibly entrapment within the soil matrix. However, the longer N_2O entrapment persists, the greater the potential for reduction to N_2 due to the declining soil redox value (Hansen et al., 2014). Based on the current results, the low ratio of the cumulative fluxes (N_2–N/N_2O-N) at D_p/D_o values of >0.005 indicate that economically significant N losses from ruminant urine patches or urea fertilizer are unlikely at D_p/D_o values of >0.005 via denitrification processes. However, if D_p/D_o values are <0.005 gaseous N emissions are likely to be dominated by N_2 and to be substantial. This implies that soil management within a grazed pasture, with respect to reducing both N_2O and N_2 emissions, should optimize soil structure (reduce soil ρ_b) and soil water contents to maximize D_p/D_o without affecting pasture growth.

The method used to measure D_p/D_o assumes O_2 consumption is negligible (Rolston and Moldrup, 2002). However, as Petersen et al. (2013) noted, D_p/D_o value is a function of both O_2 supply and demand. Using calculated D_p/D_o values, Petersen et al. (2013) measured N_2O emissions occurring in cropping soils following NO_3^- addition when D_p/D_o values were >0.02, possibly as a result of a freeze–thaw cycle releasing labile C, which they speculated may have in turn induced a high O_2 demand, suboxic conditions, and subsequent denitrification. In the current study, it is also highly likely the O_2 demand was elevated as a consequence of the urea application increasing DOC concentrations since the ensuing high soil pH that follows urea application induces the solubilization of soil organic matter (Monaghan and Barraclough, 1993). The strong correlations observed between soil pH and DOC concentrations support solubilization of soil organic matter as the DOC source. While the soil DOC concentrations declined with time in all soil ρ_b treatments, they remained above the minimum value required for denitrification to commence, previously reported to be 40 mg C kg^{-1} soil (Beauchamp et al., 1980). Oxygen consumption and availability in a soil may also be driven by soil temperature, which determines respiration rates (Smith et al., 2003). While a D_p/D_o value of 0.02 has been reported as a boundary for development of anaerobiosis (Stepniewski, 1981), the current results where N_2 production occurred at a D_p/D_o of 0.026, albeit at a lower rate, and those of Petersen et al. (2013) demonstrate deni-

trification mechanisms occurring at D_p/D_o values of >0.02. This indicates that either anaerobiosis is developing at D_p/D_o values of >0.02 and/or the mechanism of N_2O and/or N_2 production may not require anoxia and may in fact be a consequence of nitrifier-denitrification, which can operate at the boundary of oxic and anoxic conditions (Wrage et al., 2001; Zhu et al., 2013). To assess the potential shift (increase) in critical D_p/D_o, with changing soil O_2 demand, future work should investigate the interaction of varying C inputs and temperature conditions on both D_p/D_o and subsequent N_2O and N_2 emissions, along with microbial processes.

CONCLUSIONS

Cumulative emissions of N_2O and N_2 over 35 d following a urea input designed to simulate a ruminant urine deposition event were affected by both soil ρ_b and ψ. For the first time, we show that cumulative emissions from such an N input can also be strongly related to soil D_p/D_o and that the rapid decline in N_2O production, as D_p/D_o decreases to exceed a critical value, is the consequence of N_2 production. Soil and irrigation management should be optimized to maximize D_p/D_o to mitigate economic and environmental losses of N. Future studies are needed to examine how soil microbes and soil O_2 supply change with varying D_p/D_o conditions as a consequence of soil management and temperature.

ACKNOWLEDGMENTS

This research was funded by the Ministry for Business, Innovation, and Employment under the Land Use Change and Intensification (C02X0812) program of the New Zealand Institute for Plant & Food Research. We thank Chris Dunlop (New Zealand Institute for Plant & Food Research), Qian Liang, Roger Cresswell, and Manjula Premaratne (Lincoln University, New Zealand) for help with analyses.

REFERENCES

Andersen, A.J., and S.O. Petersen. 2009. Effects of C and N availability and soil-water potential interactions on N_2O evolution and PLFA composition. Soil Biol. Biochem. 41:1726–1733. doi:10.1016/j.soilbio.2009.06.001

Anderson, T.W., and D.A. Darling. 1952. Asymptotic theory of certain "Goodness of Fit" criteria based on stochastic processes. Ann. Math. Stat. 23:193–212. doi:10.1214/aoms/1177729437

Avnimelech, Y., and M. Laher. 1977. Ammonia volatilization from soils: Equilibrium considerations. Soil Sci. Soc. Am. J. 41:1080–1084. doi:10.2136/sssaj1977.03615995004100060013x

Balaine, N., T.J. Clough, M.H. Beare, S.M. Thomas, E.D. Meenken, and J.G. Ross. 2013. Changes in relative gas diffusivity explain soil nitrous oxide flux dynamics. Soil Sci. Soc. Am. J. 77:1496–1505. doi:10.2136/sssaj2013.04.0141

Ball, B.C. 2013. Soil structure and greenhouse gas emissions: A synthesis of 20 years of experimentation. Eur. J. Soil Sci. 64:357–373. doi:10.1111/ejss.12013

Bathurst, N.O. 1952. The amino acids of sheep and cow urine. J. Agric. Sci. (Cambridge) 42:476–478. doi:10.1017/S0021859600057385

Beauchamp, E.G., C. Gale, and J.C. Yeomans. 1980. Organic matter availability for denitrification in soils of different textures and drainage classes. Commun. Soil Sci. Plant Anal. 11:1221–1233. doi:10.1080/00103628009367119

Blakemore, L.C., P.L. Searle, and B.K. Daly. 1987. Methods for chemical analysis of soils. Manaaki-Whenua Press, Lincoln, New Zealand.

Buckthought, L.E., T.J. Clough, K.C. Cameron, H.J. Di, and M.A. Shepherd. 2015. Urine patch and fertiliser N interaction: Effects of fertiliser rate and season of urine application on nitrate leaching and pasture N uptake. Agric. Ecosyst. Environ. 203:19–28. doi:10.1016/j.agee.2015.01.019

Castellano, M.J., J.P. Schmidt, J.P. Kaye, C. Walker, C.B. Graham, H.M. Lin, and C.J. Dell. 2010. Hydrological and biogeochemical controls on the timing and magnitude of nitrous oxide flux across an agricultural landscape. Glob. Change Biol. 16:2711–2720. doi:10.1111/j.1365-2486.2009.02116.x

Clough, T.J., F.M. Kelliher, Y.P. Wang, and R.R. Sherlock. 2006. Diffusion of ^{15}N-labelled N_2O into soil columns: A promising method to examine the fate of N_2O in subsoils. Soil Biol. Biochem. 38:1462–1468. doi:10.1016/j.soilbio.2005.11.002

Clough, T.J., J.L. Ray, L.E. Buckthought, J. Calder, D. Baird, M. O'Callaghan, R.R. Sherlock, and L.M. Condron. 2009. The mitigation potential of hippuric acid on N_2O emissions from urine patches: An in situ determination of its effect. Soil Biol. Biochem. 41:2222–2229. doi:10.1016/j.soilbio.2009.07.032

Clough, T.J., R.R. Sherlock, K.C. Cameron, and S.F. Ledgard. 1996. Fate of urine nitrogen on mineral and peat soils in New Zealand. Plant Soil 178:141–152. doi:10.1007/BF00011172

Clough, T.J., R.R. Sherlock, K.C. Cameron, R.J. Stevens, R.J. Laughlin, and C. Muller. 2001. Resolution of the ^{15}N balance enigma? Aust. J. Soil Res. 39:1419–1431. doi:10.1071/SR00092

Cook, F.J., J.H. Knight, and F.M. Kelliher. 2013. Modelling oxygen transport in soil with plant root and microbial oxygen consumption: Depth of oxygen penetration. Soil Res. 51:539–553. doi:10.1071/SR13223

Davidson, E.A. 2009. The contribution of manure and fertilizer nitrogen to atmospheric nitrous oxide since 1860. Nat. Geosci. 2:659–662. doi:10.1038/ngeo608

de Klein, C.A.M., R.R. Sherlock, K.C. Cameron, and T.J. van der Weerden. 2001. Nitrous oxide emissions from agricultural soils in New Zealand: A review of current knowledge and directions for future research. J. R. Soc. N. Z. 31:543–574. doi:10.1080/03014223.2001.9517667

Delgado, J.A. 2002. Quantifying the loss mechanisms of nitrogen. J. Soil Water Conserv. 57:389–398.

Dobbie, K., I.P. McTaggart, and K.A. Smith. 1999. Nitrous oxide emissions from intensive agriculture systems: Variations between crops and seasons, key driving variables and mean emission factors. J. Geophys. Res. 104:26891–26899. doi:10.1029/1999JD900378

Dobbie, K., and K.A. Smith. 2001. The effects of temperature, water-filled pore space and land use on N_2O emissions from an imperfectly drained gleysol. Eur. J. Soil Sci. 52:667–673. doi:10.1046/j.1365-2389.2001.00395.x

Farquharson, R., and J. Baldock. 2008. Concepts in modelling N_2O emissions from land use. Plant Soil 309:147–167. doi:10.1007/s11104-007-9485-0

Flury, M., and H. Fluhler. 1994. Brilliant blue FCF as a dye tracer for solute transport studies: A toxicological overview. J. Environ. Qual. 23:1108–1112. doi:10.2134/jeq1994.00472425002300050037x

Ghani, A., M. Dexter, and K.W. Perrott. 2003. Hot-water extractable carbon in soils: A sensitive measurement for determining impacts of fertilisation, grazing and cultivation. Soil Biol. Biochem. 35:1231–1243. doi:10.1016/S0038-0717(03)00186-X

Hansen, M., T.J. Clough, and B. Elberling. 2014. Flooding-induced N_2O emission bursts controlled by pH and nitrate in agricultural soils. Soil Biol. Biochem. 69:17–24. doi:10.1016/j.soilbio.2013.10.031

Harrison-Kirk, T., S.M. Thomas, T.J. Clough, M.H. Beare, T.J. van der Weerden, and E.D. Meenken. 2015. Compaction influences N_2O and N_2 emissions from ^{15}N-labeled synthetic urine in wet soils during successive saturation/drainage cycles. Soil Biol. Biochem. 88:178–188. doi:10.1016/j.soilbio.2015.05.022

Haynes, R.J., and P.H. Williams. 1993. Nutrient cycling and soil fertility in the grazed pasture ecosystem. Adv. Agron. 49:119–199. doi:10.1016/S0065-2113(08)60794-4

Hewitt, A.E. 1998. New Zealand soil classification. Landcare research science series no. 1. 2nd ed. Manaaki Whenua Press, Lincoln, New Zealand.

Hutchinson, G.L., and A.R. Mosier. 1981. Improved soil cover method for field measurement of nitrous oxide fluxes. Soil Sci. Soc. Am. J. 45:311–316. doi:10.2136/sssaj1981.03615995004500020017x

Klefoth, R.R., T.J. Clough, O. Oenema, and J.W. van Groenigen. 2014. Soil bulk density and moisture content influence relative gas diffusivity and the reduction of nitrogen-15 nitrous oxide. Vadose Zone J. 13:1–8. doi:10.2136/vzj2014.07.0089

Kool, D.M., E. Hoffland, S.P.A. Abrahamse, and J.W. van Groenigen. 2006. What artificial urine composition is adequate for simulating soil N_2O fluxes and mineral N dynamics? Soil Biol. Biochem. 38:1757–1763. doi:10.1016/j.soilbio.2005.11.030

Letey, J., W.A. Jury, A. Hadas, and N. Valoras. 1980. Gas diffusion as a factor in

laboratory incubation studies on denitrification. J. Environ. Qual. 9:223–227. doi:10.2134/jeq1980.00472425000900020012x

Linn, D.M., and J.W. Doran. 1984. Effect of water-filled pore space on carbon dioxide and nitrous oxide production in tilled and nontilled soils. Soil Sci. Soc. Am. J. 48:1267–1272. doi:10.2136/sssaj1984.03615995004800060013x

Maharjan, B., and R.T. Venterea. 2013. Nitrite intensity explains N management effects on N_2O emissions in maize. Soil Biol. Biochem. 66:229–238. doi:10.1016/j.soilbio.2013.07.015

McTaggart, I.P., H. Akiyama, H. Tsuruta, and B.C. Ball. 2002. Influence of soil physical properties, fertiliser type and moisture tension on N_2O and NO emissions from nearly saturated Japanese upland soils. Nutr. Cycl. Agroecosyst. 63:207–217. doi:10.1023/A:1021119412863

Millington, R.J., and J.P. Quirk. 1961. Permeability of porous solids. Trans. Faraday Soc. 57:1200–1207.

Moldrup, P., J.E. Olesen, P. Schjønning, T. Yamaguchi, and D.E. Rolston. 2000. Predicting the gas diffusion coefficient in undisturbed soil from soil water characteristics. Soil Sci. Soc. Am. J. 64:94–100. doi:10.2136/sssaj2000.64194x

Monaghan, R.M., and D. Barraclough. 1993. Nitrous oxide and dinitrogen emissions from urine-affected soil under controlled conditions. Plant Soil 151:127–138. doi:10.1007/BF00010793

Morley, N., E. Baggs, P. Dörsch, and L. Bakken. 2008. Production of NO, N_2O and N_2 by extracted soil bacteria, regulation by NO_2^- and O_2 concentrations. FEMS Microbiol. Ecol. 65:102–112. doi:10.1111/j.1574-6941.2008.00495.x

Mosier, A.R., J.K. Syers, and J.R. Freney. 2004. Nitrogen fertilizer: An essential component of icreased food, feed, and fiber production. In: A.R. Mosier et al., editors, Agriculture and the nitrogen cycle. Assessing the impacts of fertilizer use on food production and the environment. Island Press, Washington, DC. p. 3–15.

Mulvaney, R.L., and C.W. Boast. 1986. Equations for determination of nitrogen-15 labeled dinitrogen and nitrous oxide by mass spectrometry. Soil Sci. Soc. Am. J. 50:360–363. doi:10.2136/sssaj1986.03615995005000020021x

Petersen, S.O., P. Ambus, L. Elsgaard, P. Schjønning, and J.E. Olesen. 2013. Long-term effects of cropping system on N_2O emission potential. Soil Biol. Biochem. 57:706–712. doi:10.1016/j.soilbio.2012.08.032

Petersen, S.O., P. Schjønning, I.K. Thomsen, and B.T. Christensen. 2008. Nitrous oxide evolution from structurally intact soil as influenced by tillage and soil water content. Soil Biol. Biochem. 40:967–977. doi:10.1016/j.soilbio.2007.11.017

Prosser, J.I. 2012. Part IV. Soil biology and biochemistry: Soil biology in its second golden age. 27.3 Nitrogen transformations. In: P.N. Huang, Y. Li, and M.E. Sumner, editors, Handbook of soil sciences: Properties and processes. 2nd ed. CRC Press, London, UK. p. 27-19–27-32.

Ravishankara, A.R., J.S. Daniel, and R.W. Portmann. 2009. Nitrous oxide (N_2O): The dominant ozone-depleting substance emitted in the 21st century. Science 326:123–125. doi:10.1126/science.1176985

Rolston, D.E., and P. Moldrup. 2002. Gas Diffusivity. In: G.C. Topp and J.H. Dane, editors, Methods of soil analysis. Part 4. Physical methods. SSSA, Madison, WI. p. 113–139.

Romano, N., J.W. Hopmans, and G.H. Dane. 2002. Water retention and storage. In: G.C. Topp and G.H. Dane, editors, Methods of soil analysis. Part 4. Physical methods. SSSA, Madison, WI. p. 692–698.

Schjønning, P., I.K. Thomsen, P. Moldrup, and B.T. Christensen. 2003. Linking soil microbial activity to water- and air-phase contents and diffusivities. Soil Sci. Soc. Am. J. 67:156–165. doi:10.2136/sssaj2003.1560

Smith, K.A., T. Ball, F. Conen, K.E. Dobbie, J. Massheder, and A. Rey. 2003. Exchange of greenhouse gases between soil and atmosphere: Interactions of soil physical and biological processes. Eur. J. Soil Sci. 54:779–791. doi:10.1046/j.1351-0754.2003.0567.x

Stepniewski, W. 1981. Oxygen diffusion and the strength as related to soil compaction. II. Oxygen diffusion coefficient. Polish J. Soil Sci. 14:3–13.

Stevens, R.J., R.J. Laughlin, G.J. Atkins, and S.J. Prosser. 1993. Automated determination of nitrogen-15 labelled dinitrogen and nitrous oxide by mass spectrometry. Soil Sci. Soc. Am. J. 57:981–988. doi:10.2136/sssaj1993.03615995005700040017x

Tiedje, J., S. Simkins, and P. Groffman. 1989. Perspectives on measurement of denitrification in the field including recommended protocols for acetylene based methods. Plant Soil 115:261–284. doi:10.1007/BF02202594

Van der Weerden, T.J., F.M. Kelliher, and C.A.M. de Klein. 2012. Influence of pore size distribution and soil water content on nitrous oxide emissions. Soil Res. 50:125–135.

Venterea, R., T.J. Clough, J.A. Coulter, and F. Breuillin-Sessoms. 2015. Ammonium sorption and ammonia inhibition of nitrite-oxidizing bacteria explain contrasting soil N_2O production. Sci. Rep. 5:12153. doi:10.1038/srep12153

Walczak, R., E. Rovdan, and B. Witkowska-Walczak. 2002. Water retention characteristics of peat and sand mixtures. Int. Agrophys. 16:161–165.

Wrage, N., G.L. Velthof, M.L. van Beusichem, and O. Oenema. 2001. Role of nitrifier denitrification in the production of nitrous oxide. Soil Biol. Biochem. 33:1723–1732. doi:10.1016/S0038-0717(01)00096-7

Zhu, X., M. Burger, T.A. Doaneb, and W.R. Howarth. 2013. Ammonia oxidation pathways and nitrifier denitrification are significant sources of N_2O and NO under low oxygen availability. Proc. Natl. Acad. Sci. USA 110:6328–6333. doi:10.1073/pnas.1219993110